IEEE Access
Multidisciplinary | Rapid Review | Open Access Journal

Received July 18, 2021, accepted July 31, 2021, date of publication August 9, 2021, date of current version August 13, 2021.

Digital Object Identifier 10.1109/ACCESS.2021.3103584

Investigation on Design of Novel Step-Up 18-Pulse Auto-Transformer Rectifier

XIAOQIANG CHEN[1,2], TAO CHEN[1], AND YING WANG[2]
[1]School of Automation and Electrical Engineering, Lanzhou Jiaotong University, Lanzhou 730070, China
[2]Opto-Technology and Intelligent Control, Ministry of Education, Lanzhou Jiaotong University, Lanzhou 730070, China

Corresponding author: Tao Chen (ct0219338@163.com)

This work was supported in part by the National Natural Science Foundation of China under Grant 51767013 and Grant 52067013, in part by the Natural Science Foundation of the Key Laboratory of Opto-Electronic Technology and Intelligent Control, Ministry of Education, under Grant KFKT2020-12, and in part by Tianyou Innovation Team Science Foundation of Intelligent Power Supply and State Perception for Rail Transit under Grant TY202010.

ABSTRACT The multi-pulse rectifier has gained a wide range of applications in the high-power rectification system due to the advantages like simple structure, high efficiency, and high reliability. In this paper, an 18-pulse auto-transformer rectifier unit (ATRU) with adjustable output DC voltage was studied, to meet the requirements of high efficiency and low harmonic pollution of ATRU. Firstly, the basic operating principle of the proposed ATRU was analyzed in detail. The essential relationship between the step-up ratio factor and the output DC voltage, the total harmonic distortion (THD) of the input line current, and the equivalent kVA rating of the transformer was deduced considerately, which provides a theoretical basis for the optimization design of the system. Finally, the correctness of the theoretical analysis was verified by simulation and experiment. The experimental results show that under the 6kVA rating condition when the step-up ratio is 1.137, the transformer equivalent kVA rating is only 27.8% of the load output power, the input line current THD of ATRU is 6.58%, and the efficiency is 98.5%.

INDEX TERMS 18-pulse, step-up ratio, auto-transformer, high power density, equivalent kVA rating.

NOMENCLATURE

ATRU	Auto-transformer rectifier unit
THD	Total harmonic distortion
VSR-ATPS	Auto-transformer for phase-shifting with variable step-up ratio
IPRs	Inter-balance reactors
SEPIC	Single-ended primary inductance converter
RMS	Root mean square
EMI	Electromagnetic interference

I. INTRODUCTION

Multi-pulse auto-transformer rectifier units (ATRUs) are widely used in motor drive systems, electrical propulsion systems for ships and power supply systems for more-electric aircraft because of many advantages such as low-cost, high efficiency, and high reliability [1]–[3]. In these applications, ATRUs are used as front-end AC/DC converters [4], [5]. Commonly, 12-, 18-, and 24-pulse ATRUs and various modified ATRUs are available. among them, 18-pulse ATRUs not only meet the harmonic requirements well but also become the focus of research and attention because of their relatively simple structure and variable winding forms.

In recent years, studies on 18-pulse auto-transformer rectifiers have mainly focused on the input-output characteristics, winding structures and the comparison of the advantages of different winding structures under two phase shifts of $\pm 37°$ and $\pm 40°$. The operating principle and implementation of ATRUs with different winding structures such as D-type, P-type, and DP-type at 37° phase-shift are discussed in [6]–[8]. According to 37° and 40° phase-shift in [9], the characteristics and advantages of different topologies (D-, P-, DP-type) are obtained by analyzing and comparing the three winding forms to meet the application requirements of different occasions. In [10], a new topology of dual 18-pulse ATRU is proposed to solve the problem of residual low harmonics such as 5th and 7th in individual phase-shifting transformer caused by phase shift errors due to fabrication and other reasons. In [11], an 18-pulse ATRU with isolated SEPIC converters is suggested to promote galvanic isolation and regulate the output voltage, making the ATRU is less sensitive to load variations or supply voltage. Ref [12], [13] described 40° phase-shift 18-pulse ATRU, wherein the transformer is capable of specific boost functions, but the step-up ratio is

The associate editor coordinating the review of this manuscript and approving it for publication was M. Venkateshkumar.

not adjustable and the equivalent kVA rating is significantly large. In order to solve the problem of non-adjustable output voltage, a variable step-up ratio 18-pulse ATRU is presented in [14]. However, the step-up range is small and the boost capacity is limited. A mathematical analysis of the 18-pulse rectifier based on phase diagrams in the D-type and W-type winding structures was carried out in [15]. The transformer configuration used has a step-up function, but the exact mathematical relationships for key indicators such as equivalent kVA rating and harmonic factor were not given., In [16], it was demonstrated through simulation experiments that the DP-type structure has a step-up function while the P-type structure has a step-down function at 37° phase-shift, but it lacks the theoretical analysis. In addition, ATRU has been studied and applied in new energy generation applications such as wind power generation [17].

In conclusion, the trend of diversification of power electronics devices has put forward some new requirements on ATRUs, such as the ability to ensure flexible and variable voltage output, or even arbitrary variable output voltage, while considering a small equivalent kVA rating. Therefore, solving the problems of large equivalent kVA rating and non-adjustable output voltage of ATRU is important for the expansion of higher power AC-DC rectifier system units.

In this paper, a variable step-up ratio 18-pulse ATRU with high power density is investigated, and its basic operation principle is analyzed in detail to demonstrate the basic relationship between step-up ratio factor and output DC voltage; the theoretical expressions of input line current and equivalent kVA rating of transformer are derived in detail, and the essential relationship between them and step-up ratio factor is quantitatively analyzed to provide theoretical support for system optimization; the cross-sectional comparison of several different structures transformer with variable step-up ratio are compared, and the equivalent kVA rating of the structure studied in this paper is the smallest with obvious advantages under the same step-up ratio condition. Finally, the simulation and experimental results verify the feasibility and correctness of the studied structure.

II. ANALYSIS OF VARIABLR STEP-UP RATIO 18-PULSE ATRU

A. CIRCUIT CONFIGURATION

Fig. 1 shows the circuit diagram of variable step-up ratio 18-pulse ATRU.

In Fig. 1, the input three-phase grid voltage (u_a, u_b, u_c), after the auto-transformer for phase-shifting with variable step-up ratio (VSR-ATPS), generates three sets of voltages to supply the three rectifier bridges (RECI, RECII, RECIII), respectively. The DC outputs of the three rectifier bridges are connected in parallel with the inter-balance reactors (IPRs) to supply the load; the IPRs are used to absorb the transient differences of the output voltages of the rectifier bridges to ensure that the three rectifier bridges can work independently.

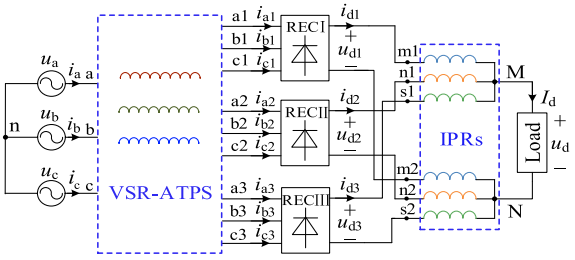

FIGURE 1. Circuit diagram of variable step-up ratio 18-pulse ATRU.

B. REQUIREMENTS OF 18-PULSE ATRU FOR THE STRUCTURE OF VSR-ATPS

1) DETERMINATION OF THE PHASE-SHIFT ANGLE

In Fig. 1, the VSR-ATPS serves to generate three sets of three-phase voltages with a certain phase difference. The phase difference is determined by the number of rectifier bridges, and the two satisfy

$$\varphi = \frac{60^\circ}{N^\circ} \tag{1}$$

where φ is the minimum phase-shift angle; N is the number of rectifier bridges.

18-pulse ATRU uses three rectifier bridges, so $\varphi = 20$. For the ATPS, the output three-phase voltage of one group connected to REC II is usually made to be in phase with the corresponding input phase voltage, and the other two groups of output three-phase voltages forward and lagging the corresponding input phase voltage by 20°, respectively, and the voltage phase diagram VSR-ATPS is shown in Fig. 2.

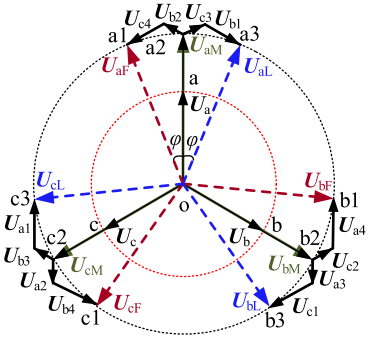

FIGURE 2. Phasor diagram of the proposed Star-type VSR-ATPS.

In Fig. 2, $\boldsymbol{U}_a$, $\boldsymbol{U}_b$ and $\boldsymbol{U}_c$ are the input phase voltages, and ($\boldsymbol{U}_{aF}$, $\boldsymbol{U}_{bF}$, $\boldsymbol{U}_{cF}$), ($\boldsymbol{U}_{aM}$, $\boldsymbol{U}_{bM}$, $\boldsymbol{U}_{cM}$) and ($\boldsymbol{U}_{aL}$, $\boldsymbol{U}_{bL}$, $\boldsymbol{U}_{cL}$) are the three sets of output phase voltages that are forward, in-phase and lagging the input phase voltages, respectively.

2) DETERMINATION OF WINDING CONFIGURATION

From Fig. 2, it can be obtained that

$$\boldsymbol{U}_{aF} = \boldsymbol{U}_{aM} + \boldsymbol{U}_{b2} + \boldsymbol{U}_{c4} \tag{2}$$

Combining Fig. 2 and (2), the output phase voltage $\boldsymbol{U}_{aF}$ is a vector synthesis of the output phase voltage $\boldsymbol{U}_{aM}$, the phasors

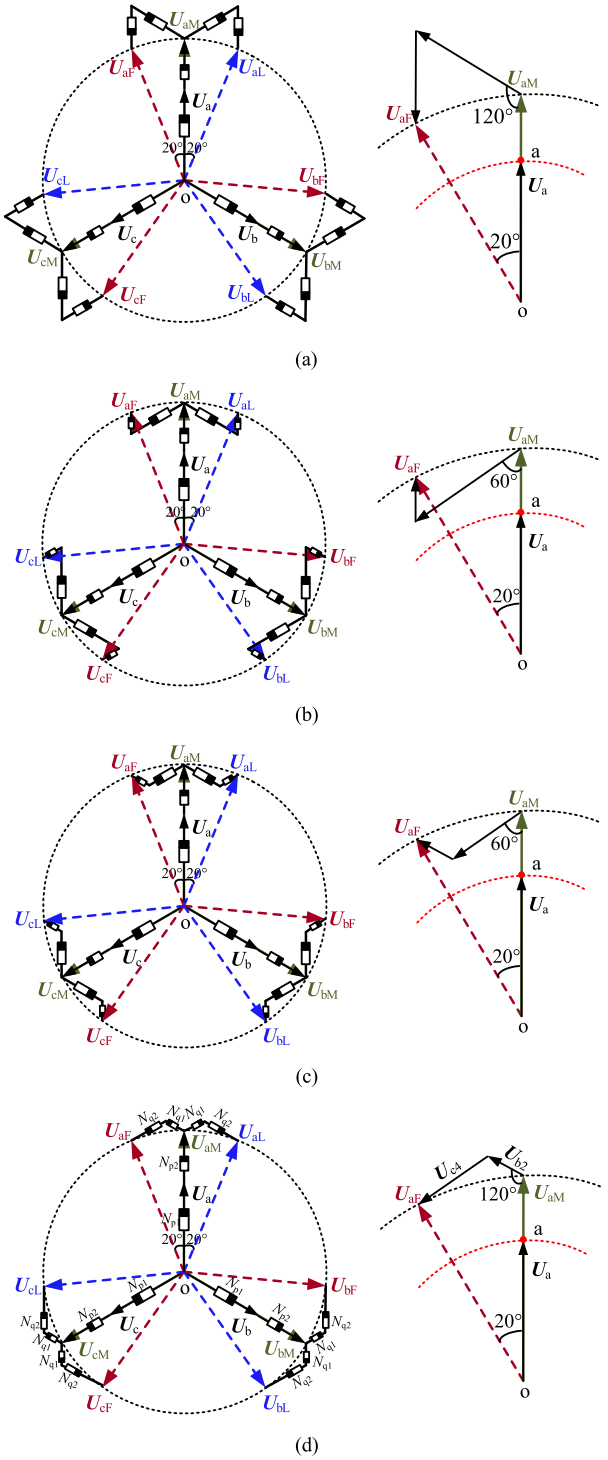

FIGURE 3. Phasor diagrams of Star-type VSR-ATPS. (a) Scheme 1. (b) Scheme 2. (c) Scheme 3. (d) Scheme 4.

$\boldsymbol{U}_{b2}$ and $\boldsymbol{U}_{c4}$. The phasors $\boldsymbol{U}_{b2}$ and $\boldsymbol{U}_{c4}$ determine the structure and kVA rating of VSR-ATPS, which are usually designed according to the principle of the simplest structure and the lowest kVA rating. Fig. 3 gives all possible configurations of the symmetric (20° phase-shift) Star-type VSR-ATPS.

As can be seen in Fig. 3, the four schemes have the same step-up principle, to save space, scheme 4 is used as an example to focus on the analysis. Fig. 4 shows the winding configuration of Scheme 4.

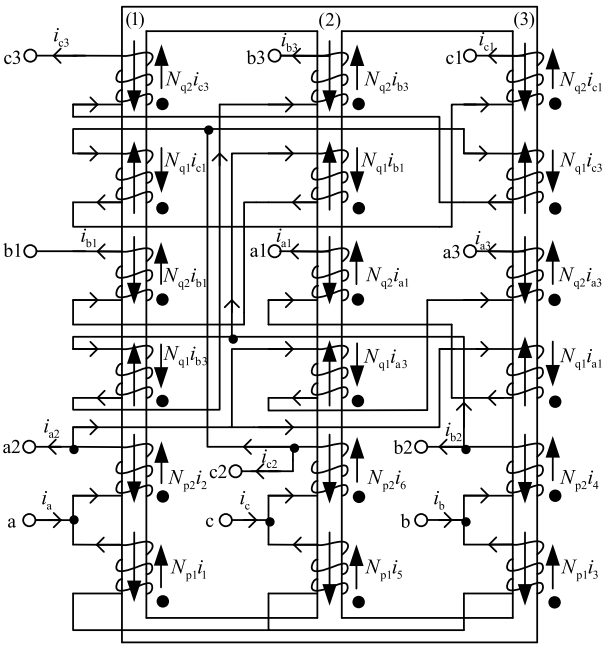

FIGURE 4. Winding configuration of Scheme 4.

Combing Fig. 2, Fig. 3(d) and Fig. 4, it can be seen that the phasors $\boldsymbol{U}_{ij}$ (i = a, b, c; $j = 1, 2, 3, 4$) are parallel to the phasors $\boldsymbol{U}_{iM}$ and $\boldsymbol{U}_{i}$; the phasors $\boldsymbol{U}_{i}$ and $\boldsymbol{U}_{iM}$ are also considered as the voltages across winding N_{p1} and $(N_{p1} + N_{p2})$, respectively; $\boldsymbol{U}_{ij}$ is the voltage across winding N_{q1} ($j = 2, 3$) and N_{q2} ($j = 1, 4$), respectively.

Suppose that the input three-phase grid voltages as

$$\begin{cases} u_a = \sqrt{2}\, U_m \sin \omega t \\ u_b = \sqrt{2}\, U_m \sin(\omega t - 120°) \\ u_c = \sqrt{2}\, U_m \sin(\omega t + 120°) \end{cases} \tag{3}$$

where U_m is the root mean square (RMS) value of the input phase voltage.

Combing the relationship between the voltages in Fig. 3(d) and (1), it can be obtained as

$$\begin{cases} u_{aF} = \sqrt{2}\, U_n \sin(\omega t + 20°) \\ u_{bF} = \sqrt{2}\, U_n \sin(\omega t - 100°) \\ u_{cF} = \sqrt{2}\, U_n \sin(\omega t + 140°) \end{cases} \tag{4}$$

$$\begin{cases} u_{aM} = \sqrt{2}\, U_n \sin \omega t \\ u_{bM} = \sqrt{2}\, U_n \sin(\omega t - 120°) \\ u_{cM} = \sqrt{2}\, U_n \sin(\omega t + 120°) \end{cases} \tag{5}$$

$$\begin{cases} u_{aL} = \sqrt{2}\, U_n \sin(\omega t - 20°) \\ u_{bL} = \sqrt{2}\, U_n \sin(\omega t - 140°) \\ u_{cL} = \sqrt{2}\, U_n \sin(\omega t + 100°) \end{cases} \tag{6}$$

where U_n is the RMS value of the output phase voltage of VSR-ATPS.

According to Fig. 3(d), the following relationship can be obtained

$$(N_{p1}+N_{p2}):N_{q1}:N_{q2}=1:k_1:k_2 \tag{7}$$

Then (2) can be transformed as

$$\mathbf{U}_{aF}=\mathbf{U}_{aM}-k_1\mathbf{U}_{bM}+k_2\mathbf{U}_{cM} \tag{8}$$

Substituting (4) and (5) into (8) yields

$$\begin{cases} k_1=0.1372 \\ k_2=0.2578 \end{cases} \tag{9}$$

Define the step-up ratio G of VSR-ATPS as

$$G=\frac{U_n}{U_m}=\frac{OU_{aM}}{OU_a}=\frac{N_{p1}+N_{p2}}{N_{p1}}=1+\frac{N_{p2}}{N_{p1}} \tag{10}$$

From Fig. 3(d), when winding turns N_{p2} to zero, the transformer step-up ratio G reaches its minimum value of 1. According to (7)-(9), once the winding turns $(N_{p1}+N_{p2})$ are determined, the step-up ratio G will keep getting larger as the winding turns N_{p2} increases and N_{p1} decreases, i.e., as the winding tap position (power access point) moves from point a2 to point O. Therefore, the value of G theoretically takes a range of [1, ∞). The step-up ratio G reflects the step-up capability of the VSR-ATPS. In addition, the 18-pulse ATRU itself has a potential boost ratio U_d/U_m (U_d is the RMS value of the output DC voltage u_d), so the output DC voltage of the proposed ATRU depends on the step-up ratio G of the VSR-ATPS.

III. OPERATION CHARACTERISTICS OF 18-ATRU

For the subsequent theoretical analysis and calculations, the following assumptions are given. 1) The leakage inductance of VSR-ATPS is ignored. 2) Diodes are the ideal devices in rectifier bridges. 3) The ATRU operates in a large inductive load state and the load current i_d can be considered as a constant I_d. Therefore, according to the symmetry of the system, it can be obtained that

$$i_{d1}=i_{d2}=i_{d3}=\frac{I_d}{3} \tag{11}$$

A. INPUT LINE CURRENT

From (7)- (10), it can be obtained

$$\frac{N_{p2}}{N_{p1}}=(G-1),\quad \frac{N_{q1}}{N_{p1}}=k_1G,\quad \frac{N_{q2}}{N_{p1}}=k_2G \tag{12}$$

In Fig. 4, According to the principle of magnetomotive force balance, it can be gained

$$\begin{cases} N_{p1}i_1+N_{p2}i_2+N_{q2}(i_{b1}+i_{c3})=N_{q1}(i_{b3}+i_{c1}) \\ N_{p1}i_3+N_{p2}i_4+N_{q2}(i_{c1}+i_{a3})=N_{q1}(i_{c3}+i_{a1}) \\ N_{p1}i_5+N_{p2}i_6+N_{q2}(i_{a1}+i_{b3})=N_{q1}(i_{a3}+i_{b1}) \end{cases} \tag{13}$$

From Kirchhoff's current law, it can be obtained

$$\begin{cases} i_2=i_{a1}+i_{a2}+i_{a3}; & i_a=i_2-i_1; \\ i_4=i_{b1}+i_{b2}+i_{b3}; & i_b=i_4-i_3; \\ i_6=i_{c1}+i_{c2}+i_{c3}; & i_c=i_6-i_5; \end{cases} \tag{14}$$

From (13) and (14), the input line current i_a is obtained as follows

$$i_a=\frac{(i_{a1}+i_{a2}+i_{a3})(N_{p1}+N_{p2})+(i_{b1}+i_{c3})N_{q2}-(i_{c1}+i_{b3})N_{q1}}{N_{p1}} \tag{15}$$

Based on modulation theory, the output current and input current of the rectifier bridges meet

$$\begin{cases} i_{a1}=S_{a1}i_{d1}; & i_{b1}=S_{b1}i_{d1}; & i_{c1}=S_{c1}i_{d1}; \\ i_{a2}=S_{a2}i_{d2}; & i_{b2}=S_{b2}i_{d2}; & i_{c2}=S_{c2}i_{d2}; \\ i_{a3}=S_{a3}i_{d3}; & i_{b3}=S_{b3}i_{d3}; & i_{c3}=S_{c3}i_{d3}; \end{cases} \tag{16}$$

where S_{a1}, S_{b1}, S_{c1}, S_{a2}, S_{b2} S_{c2}, S_{a3}, S_{b3} and S_{c2} are switching functions corresponding to phases a1, b1, c1, a2, b2, c2, a3, b3 and c3. Among them, the phase diagram of the S_{a2} is shown in Fig. 5.

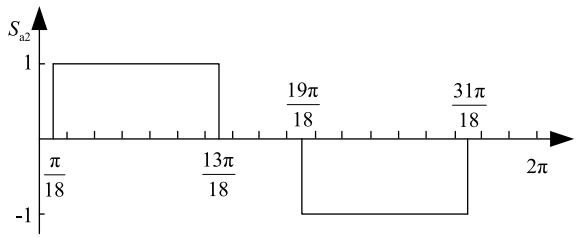

FIGURE 5. Phase diagram of the switching function S_{a2}.

The relationship between the switching functions meet

$$\begin{cases} S_{a1}=S_{a2}\angle 20^\circ; & S_{b1}=S_{a2}\angle -100^\circ; \\ & S_{c1}=S_{a2}\angle 140^\circ; \\ S_{b2}=S_{a2}\angle -120^\circ; & S_{c2}=S_{a2}\angle 120^\circ; \\ S_{a3}=S_{a2}\angle -20^\circ; & S_{b3}=S_{a2}\angle -140^\circ; \\ & S_{c3}=S_{a2}\angle 100^\circ; \end{cases} \tag{17}$$

Substituting (11), (16) and (17) into (5) yields

$$i_a=\frac{GI_d}{3}\left[(S_{a1}+S_{a2}+S_{a3})+k_2(S_{b1}+S_{c3})-k_1(S_{c1}+S_{b3})\right] \tag{18}$$

According to (18), the theoretical waveform of input line current i_a is obtained, as shown in Fig. 6.

In Fig. 6, it is noticed that input line current exhibits 18-step waves in one power supply cycle, so the designed ATRU can achieve 18-pulse rectification when analyzed from the input-side of ATRU.

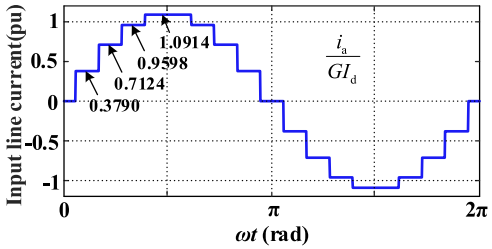

FIGURE 6. Theoretical waveform of input line current of phase a.

From Fig. 6, the RMS value of input line current i_a can be calculated as

$$I_a = \sqrt{\frac{2}{9}(0.3790^2 + 0.7124^2 + 0.9598^2 + 1.0914^2)}GI_d = 0.7837GI_d \tag{19}$$

Using the midpoint of i_a positive waveform and the negative waveform as the zero moment, its Fourier series expansion is deduced as

$$i_a = \sum_{n=1,17,19\cdots}^{\infty} \frac{4GI_d}{n\pi}(0.3790\cos\frac{n\pi}{18} + 0.3334\cos\frac{3n\pi}{18} + 0.2474\cos\frac{5n\pi}{18} + 0.1316\cos\frac{7n\pi}{18})\sin n\omega t \tag{20}$$

From (20), when $n = 1$, the RMS value of the fundamental current of i_a is calculated as

$$I_{af} = 0.7797GI_d \tag{21}$$

Then, the THD of the input line current is obtained as

$$i_{a\text{-THD}} = \frac{\sqrt{I_a^2 - I_{af}^2}}{I_{af}} = 10.1\% \tag{22}$$

The results of (22) indicates that the THD of input line current in proposed 18-pulse ATRU does not vary with the step-up ratio G, but always remains at about 10.1%.

B. OUTPUT DC VOLTAGE

The output voltages of the three rectifier bridges can be expressed as

$$\begin{cases} u_{d1} = S_{a1}u_{a1} + S_{b1}u_{b1} + S_{c1}u_{c1} \\ u_{d2} = S_{a2}u_{a2} + S_{b2}u_{b2} + S_{c2}u_{c2} \\ u_{d3} = S_{a3}u_{a3} + S_{b3}u_{b3} + S_{c3}u_{c3} \end{cases} \tag{23}$$

In Fig. 1, suppose the potentials at points m1, n1, s1, m2, n2, and s2 are v_{m1}, v_{n1}, v_{s1}, v_{m2}, v_{n2}, and v_{s2}, respectively, then there is

$$\begin{cases} u_{d1} = v_{m1n} - v_{m2n} \\ u_{d2} = v_{n1n} - v_{n2n} \\ u_{d3} = v_{s1n} - v_{s2n} \end{cases} \tag{24}$$

The potential at points M and N can be expressed as

$$\begin{cases} v_{Mn} = \frac{1}{3}(v_{m1n} + v_{n1n} + v_{s1n}) \\ v_{Nn} = \frac{1}{3}(v_{m2n} + v_{n2n} + v_{s2n}) \end{cases} \tag{25}$$

From (24) and (25), the output voltage u_d can be derived as

$$u_d = v_{Mn} - v_{Nn} = \frac{1}{3}(v_{m1n} - v_{m2n}) + \frac{1}{3}(v_{n1n} - v_{n2n}) + \frac{1}{3}(v_{s1n} - v_{s2n}) = \frac{1}{3}(u_{d1} + u_{d2} + u_{d3}) \tag{26}$$

According to (23), it can be obtained

$$\begin{cases} u_{d1} = \sqrt{6}\,GU_m\sin(\omega t - 10^\circ - k60^\circ) \\ \omega t \in [k60^\circ + 50^\circ, k60^\circ + 110^\circ], \quad k = 0, 1, 2\cdots, \\ u_{d2} = \sqrt{6}\,GU_m\sin(\omega t + 30^\circ - k60^\circ) \\ \omega t \in [k60^\circ + 10^\circ, k60^\circ + 70^\circ], \quad k = 0, 1, 2\cdots, \\ u_{d3} = \sqrt{6}\,GU_m\sin(\omega t + 10^\circ - k60^\circ) \\ \omega t \in [k60^\circ + 30^\circ, k60^\circ + 90^\circ], \quad k = 0, 1, 2\cdots, \end{cases} \tag{27}$$

where $k = 0, 1, 2, 3\ldots$

Therefore, the output DC voltage can be expressed as

$$\begin{aligned} u_d &= 2.351GU_m\sin(\omega t + 50^\circ - k20^\circ) \\ \omega t &\in [k20^\circ + 10^\circ, (k+1)20^\circ + 10^\circ] \end{aligned} \tag{28}$$

According to (28), the theoretical waveform of output DC voltage u_d is plotted in Fig. 7.

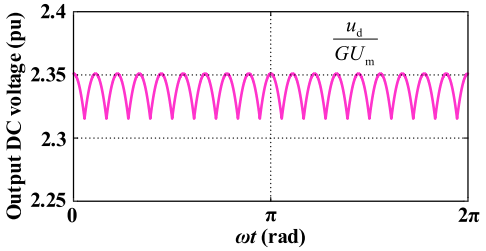

FIGURE 7. Theoretical waveform of output DC voltage.

In Fig. 7, it is noticed that the output DC voltage contains 18 equal-width waves in one power supply cycle, so the designed ATRU can achieve 18-pulse rectification when analyzed from the output-side of ATRU.

C. KVA RATING OF VSR-ATPSDC

From the above analysis for Scheme4, it can be obtained that the RMS value of voltage across windings N_{p1}, N_{p1}, N_{q1} and N_{q2} is U_m, $(G-1)\,U_m$, k_1GU_m, k_2GU_m, respectively.

Taking i_{a1} as an example, the current flowing through windings N_{q1} and N_{q2} can be expressed as

$$i_{a1} = \frac{1}{3}S_{a1}I_d \tag{29}$$

TABLE 1. The key technical indicators of typical 18-pulse VSR-ATPS.

Scheme/Ref.	Structure of VSR-ATPS	Phase shift angle φ	Step-up G	kVA of rating (%)	
				G=1	G=1.137
W(40°)/[15]	Symmetric Wye	±40°	[1, 2.53]	54.8	59.7
D(40°)/[12]	Symmetric Delta	±40°	[1, 2]	50.4	59.2
P(37°)/[12]	Asymmetric Polygon	±37°	[1, 1.42]	36	43.6
DP((37°)/[16]	Asymmetric Delta-Polygon	±37°	[1, 1.53]	27.1	34.01
Scheme 4(20°)	Symmetric Star	±20°	[1, ∞)	17.38	27.88

The RMS value of windings current i_{a1} is calculated as

$$I_{a1} = 0.2722 I_d \tag{30}$$

From (12) and (13), the current i_1 across winding N_{p1} is given by

$$i_1 = \frac{I_d}{3}\left[(G-1)(S_{a1}+S_{a2}+S_{a3}) + k_2 G(S_{b1}+S_{c3}) - k_1(S_{c1}+S_{b3})\right] \tag{31}$$

The RMS value of current i_1 is calculated as

$$I_1 = 0.7836(G-0.9618) I_d \tag{32}$$

Similarly, the RMS value of current i_2 across winding N_{p2} is obtained as

$$I_2 = 0.7537 I_d \tag{33}$$

From (28), the RMS value of the output DC voltage can be calculated as

$$U_d = 2.339 G U_m \tag{34}$$

Based on the above results, the kVA rating of the VSR-ATPS can be obtained as

$$S_{auto} = 3 \times \frac{I_d}{2}\left[U_m \times 0.7836(G-0.9618) + (G-1)U_m \times 0.7537 + 2 \times (k_1 G U_m + k_2 G U_m) \times 0.2722\right] \tag{35}$$

Define the load power as

$$P_0 = U_d I_d \tag{36}$$

According to (34)-(36), the equivalent kVA rating of VSR-ATPS is obtained as

$$S_{eq\text{-}auto} = \frac{S_{auto}}{P_0} = \frac{2.6294G - 2.262}{2.339G} \tag{37}$$

From (37), the relationship curves between the equivalent kVA rating of VSR-ATPS and the step-up ratio factor G for each of the four proposed schemes are obtained by applying the same analysis method, as shown in Fig. 8.

It is obvious from Fig. 8 that the common feature of the proposed four schemes is that the equivalent kVA rating of VSR-ATPS increases rapidly with increasing G when $1 \leq G < 5$, increases slowly with increasing G when $5 \leq G < 15$, and remains essentially constant at about 110% with increasing G when $G > 15$. However, it should be noted that at any same step-up ratio, the equivalent kVA rating of Scheme 3 and Scheme 4 are equal and their values are significantly smaller than those of Scheme 1 and Scheme 2. When the step-up ratio $G = 1$ (no step-up case), the equivalent kVA rating

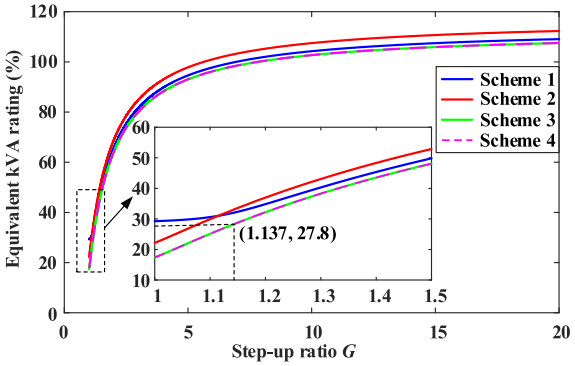

FIGURE 8. The relationship between equivalent kVA rating and step-up ratio *G* of VSR-IPR.

of Scheme 1, Scheme 2, Scheme 3, and Scheme 4 account for 29.26%, 22.17%, 17.38% and 17.38% of the load power, respectively; when $G = 15$, they account for 111%, 107.8%, 105.9% and 105.9%, respectively. Therefore, by the above analysis, Scheme 3 and Scheme 4 are optimal among the proposed four star-type VSR-ATPS structures in practical applications.

Table 1 summarizes the key performance indicators of several typical 18-pulse VSR-ATPSs. Also, to better clarify their characteristics, the equivalent kVA rating of the VSR-ATPS is further calculated and simulated when the step-up ratio G is varied from between 1 and 1.6. The results are plotted in Fig. 9.

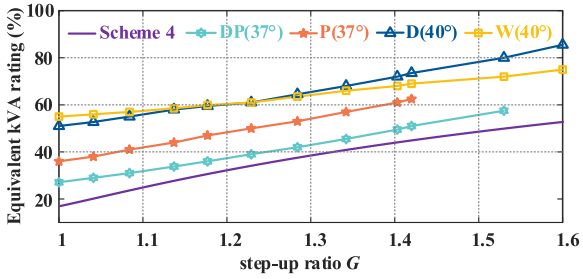

FIGURE 9. The Relationship curve of equivalent kVA rating of VSR-ATPS and the step-up ratio *G* of VSR-IPR for various structures.

From Table 1 and Fig. 9, it is known that the proposed scheme possesses the following advantages.

(1) The VSR-ATPS has a voltage-symmetric (20° phase-shift) design, which is not only simple in structure but also avoids additional non-characteristic order harmonics [14].

(2) It has the widest step-up range, which improved the flexibility of ATRU.

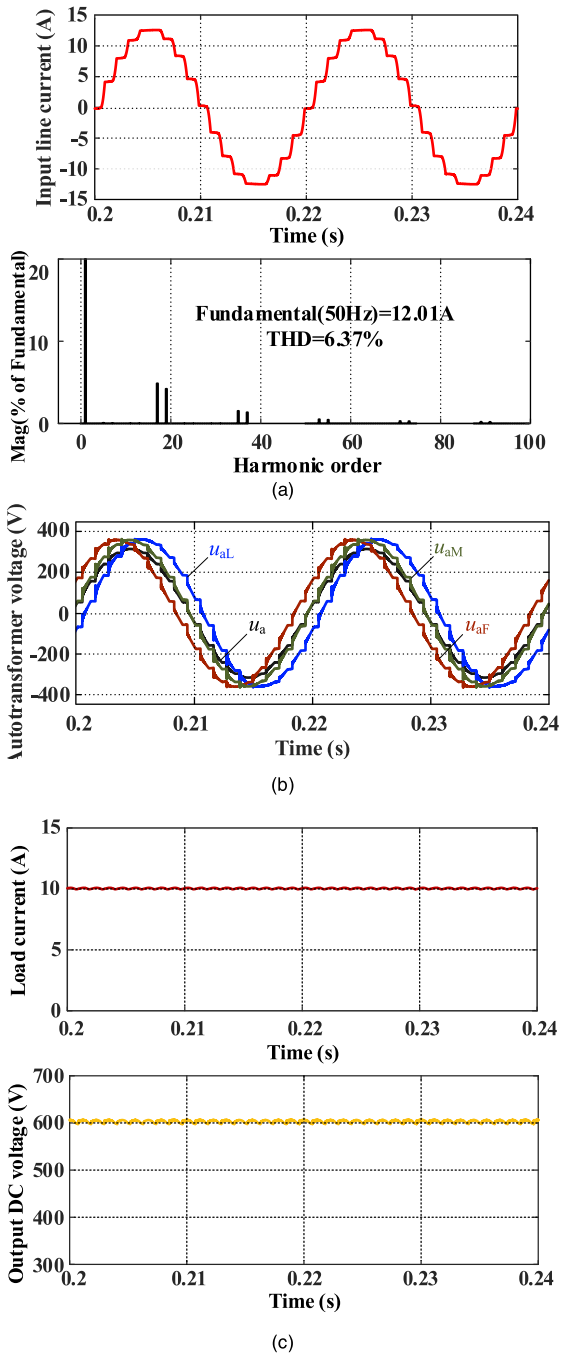

FIGURE 10. Simulation results. (a) a-phase input line current and its spectrum. (b) Input and output voltage of autotransformer. (c) load current and output DC voltage.

(3) The equivalent kVA rating is smaller than other structures with the same step-up ratio, which has a significant size and weight advantage.

IV. SIMULATION AND EXPERIMENTAL ANALYSIS

A. DESIGN SPECTIFICATIONS

The main parameters of the 18-pulse ATRU based on Scheme 4 in this paper are given in Table 2. According to the requirement, the step-up ratio $G = 1.137$ can be obtained, and further substituting it into (35) yields the equivalent kVA rating of VSR-ATPS as $S_{\text{auto}} = 1.67$ kVA, which is 27.8% of the actual output power.

TABLE 2. Design specifications.

Parameter	Symbol	Value
Rate Input voltage	U_{in}	226V
Supply frequency	f	50Hz
Rate output power	P_0	6 kVA
Input current THD	THD	<10%
full load efficiency	η	97%

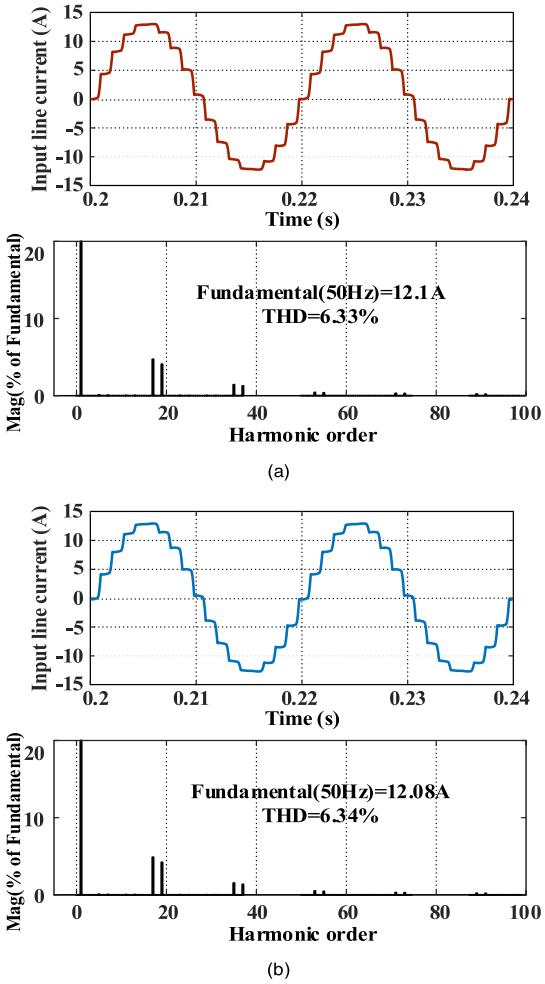

FIGURE 11. Simulation results of a-phase input line current and its spectrum. (a) Waveforms of output 500 V working condition. (b) Waveforms of output 300V working condition.

B. SIMULATION ANALYSIS

A star-type variable step-up ratio 18-pulse ATRU circuit is built by MATLAB/Simulink simulation software. Through simulation and comparison, the input filter inductance parameter is $L_{\text{in}} = 20\mu$H; the VSR-ATPS leakage inductance parameter is set to 0.02pu; resistive inductive load parameters are $R_{\text{d}} = 30$ and $L_{\text{d}} = 10$mH.

The simulation results are shown in Fig. 10. As can be seen from Fig. 10(a), the input line current i_{a} of the proposed 18-pulse ATRU presents 18 steps in a power cycle (0.02s), and the THD value is 6.37%. Therefore, from the input side, the designed ATRU realizes an 18-pulse rectifier.

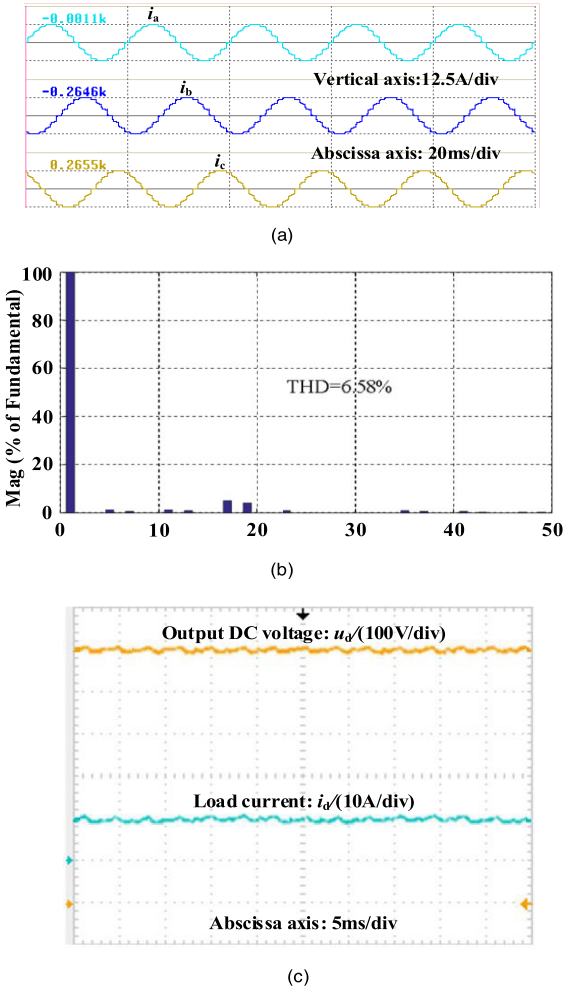

FIGURE 12. Experimental results. (a) Three-phase input line current. (b) Spectrum of a-phase input line current. (c) load current and output DC voltage voltage.

Fig. 10(b) indicates that the VSR-ATPS achieves the desired boost function. It can be seen from Fig. 10 (c) that under the large inductive load, both the output DC voltage and the load current contain 18 equal-width waves in one cycle. Therefore, from the output side, the designed ATRU also realizes an 18-pulse rectifier.

C. HARMONIC COMPARISON UNDER ADGUSTABLE OUTPUT DC VOLTAGE CONDITIONS

To illustrate that the harmonic content of the input current remains basically the same under different output DC voltage conditions, simulations were carried out for 500 V and 300 V output DC voltage conditions under the rated conditions in Table 2, and the results are shown in Fig. 11.

Combining Fig. 11 and 10(a), it is known that the input current maintains a sinusoidal trend stepwise variation under the operating conditions of 600 V, 500 V and 300 V output DC voltage, respectively, and its THD remains basically unchanged at about 6.4%, which is smaller than the theoretical value, due to the influence of the input filter inductor and the VSR-ATPS leakage inductance. The above

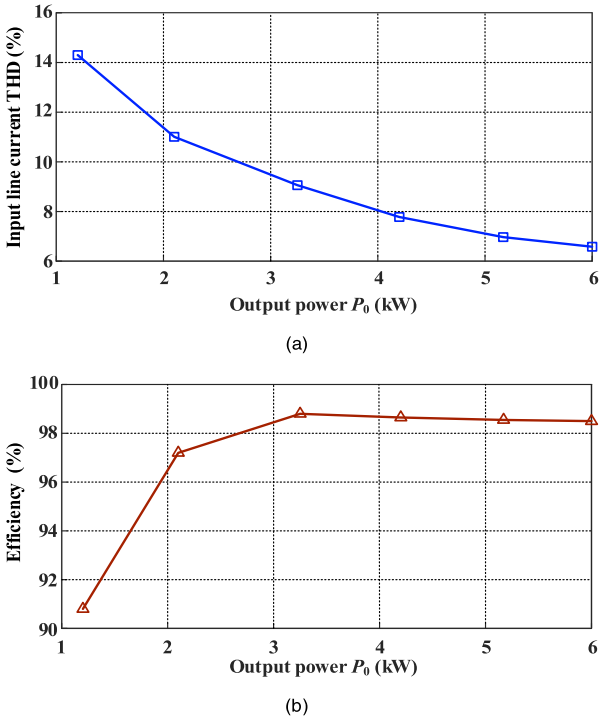

FIGURE 13. Measured THD and efficiency curves. (a) THD curve of the system. (b) efficiency curve of the system.

simulation comparison shows that the THD of the input current is basically unaffected in the case of adjustable output DC voltage, which is consistent with the results of the theoretical analysis of (22).

D. EXPERIMENTAL VERIFICATION

Based on the theoretical analysis and simulation results, a 6kVA three-phase prototype of variable step-up ratio 18-pulse ATRU was established according to Scheme 4, as shown in Fig. 12. The electromagnetic interference (EMI) filter is used on the input side of the ATRU during the experiment.

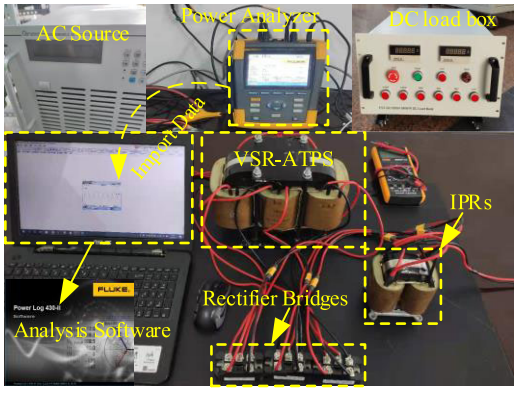

Fig. 12(a) shows the waveform of the three-phase input line current and the spectrum of the a-phase input line current under rated load conditions. It can be seen from Fig. 12(a) that the three-phase input currents are basically balanced, and the phase difference between them is 120°, and amplitudes

are about 12.5 A. The input line current mainly contains 18k ± 1th characteristic harmonic, which is consistent with the theoretical analysis. As seen in Fig. 12(b), the output DC voltage and load current are around 601 V and 10 A, respectively, and they both contain 18 pluses in one cycle, but the waveforms of output voltage and load current do not look as standard as theoretically owing to the effect of VSR-ATPS leakage inductance.

Fig. 13 gives the curves of measured THD and efficiency at full load conditions. It can be seen from Fig. 13 that the THD of the input line current of the system at full load is 6.58% and the system efficiency reaches 98.5%. The experimental results are consistent with the theoretical analysis results, and they all meet the design specifications.

V. CONCLUSION

In this paper, a star-type 18-pulse ATRU with variable step-up ratio is studied. Taking the step-up ratio G as the starting point, the essential relationship between G and output DC voltage, input current THD and equivalent kVA rating of VSR-ATPS is analyzed in detail, and it is verified by comparison that the structure studied has an obvious size and weight advantages and wide application prospects, and the following conclusions are drawn.

(1) The output DC voltage of the ATRU can be adjusted arbitrarily with a theoretical boost range of $[1, \infty)$.

(2) The adjustment of the output DC voltage has almost no effect on the THD of the input line current, and the THD can all meet the conventional requirements.

(3) The higher the output DC voltage is, the larger the equivalent kVA rating of the transformer is. While at the same step-up ratio, the equivalent kVA rating of the structure studied in this paper is significantly smaller than that of the other similar structures.

(4) The proposed VSR-ATPS adopts a voltage-symmetric design scheme, which is less likely to contribute additional non-characteristic order harmonics in the input line current, and this feature is better than that of the voltage-asymmetric design scheme.

REFERENCES

[1] Q. Du, L. Gao, Q. Li, T. Li, and F. Meng, "Harmonic reduction methods at DC side of parallel-connected multipulse rectifiers: A review," *IEEE Trans. Power Electron.*, vol. 36, no. 3, pp. 2768–2782, Mar. 2021.

[2] B. Singh, S. Gairola, B. N. Singh, A. Chandra, and K. Al-Haddad, "Multipulse AC–DC converters for improving power quality: A review," *IEEE Trans. Power Electron.*, vol. 23, no. 1, pp. 260–281, Jan. 2008.

[3] Y. Zhang, Z. Chen, B. Li, and Y. He, "Application of low harmonic 18-pulse rectifier power supply for radar power system," *IEEE Trans. Ind. Electron.*, vol. 66, no. 2, pp. 1080–1088, Feb. 2019.

[4] P. S. Prakash, R. Kalpana, and B. Singh, "Inclusive design and development of front-end multiphase rectifier with reduced magnetic rating and improved efficiency," *IEEE J. Emerg. Sel. Topics Power Electron.*, vol. 8, no. 3, pp. 2989–3000, Sep. 2020.

[5] M. Swamy, T. J. Kume, and N. Takada, "A hybrid 18-pulse rectification scheme for diode front-end rectifiers with large DC-bus capacitor," *IEEE Trans. Ind. Appl.*, vol. 46, no. 6, pp. 2484–2494, Nov. 2010.

[6] S. Khan, X. Zhang, M. Saad, H. Ali, B. M. Khan, and H. Zaman, "Comparative analysis of 18-pulse autotransformer rectifier unit topologies with intrinsic harmonic current cancellation," *Energies*, vol. 11, no. 6, p. 1347, 2018.

[7] B. Singh, G. Bhuvaneswari, and V. Garg, "A novel polygon based 18-pulse AC–DC converter for vector controlled induction motor drives," *IEEE Trans. Power Electron.*, vol. 22, no. 2, pp. 488–497, Mar. 2007.

[8] D. Wang, X. Zou, and Q. Dai, "Research on DP type airborne high-power autotransformer based on 18-pulse rectifier," *Power Electron.*, vol. 47, no. 5, pp. 65–66, May 2013.

[9] R. Burgos, A. Uan-Zo-Li, F. Lacaux, F. Wang, and D. Boroyevich, "Analysis and experimental evaluation of symmetric and asymmetric 18-pulse autotransformer rectifier topologies," in *Proc. Power Convers. Conf. Nagoya*, Apr. 2007, pp. 2–5.

[10] W. H. Hu, P. G. Song, and G. Cheng, "Characteristic of novel dual 18-pulse rectifier topology," *High Voltage Eng.*, vol. 36, no. 5, pp. 1299–1304, May 2010.

[11] A. C. Lourenco, F. J. M. Seixas, J. C. Pelicer, and P. S. Oliveira, "18-pulse autotransformer rectifier unit using SEPIC converters for regulated DC-bus and high frequency isolation," in *Proc. IEEE 13th Brazilian Power Electron. Conf. 1st Southern Power Electron. Conf. (COBEP/SPEC)*, Nov. 2015, pp. 1–6.

[12] S. Khan, G. Z. Hui, H. Ali, K. Habib, and I. U. Haq, "Comparative analysis of differential delta configured 18-pulse ATRU," in *Proc. Int. Conf. Electr. Syst. Aircr., Railway, Ship Propuls. Road Vehicles (ESARS)*, Mar. 2015, pp. 1–6.

[13] A. Uan-Zo-li, R. P. Burgos, F. Lacaux, A. Roshan, F. Wang, and D. Boroyevich, "Analysis of new step-up and step-down direct symmetric 18-pulse topologies for aircraft autotransformer-rectifier units," in *Proc. IEEE 36th Power Electron. Spec. Conf.*, Jun. 2005, pp. 1142–1148.

[14] J. Chen, Y. Shen, J. Chen, H. Bai, C. Gong, and F. Wang, "Evaluation on the autoconfigured multipulse AC/DC rectifiers and their application in more electric aircrafts," *IEEE Trans. Transport. Electrific.*, vol. 6, no. 4, pp. 1721–1739, Dec. 2020.

[15] R. C. Fernandes, P. da Silva Oliveira, and F. J. M. de Seixas, "A family of autoconnected transformers for 12- and 18-pulse converters—Generalization for delta and Wye topologies," *IEEE Trans. Power Electron.*, vol. 26, no. 7, pp. 2065–2078, Jul. 2011.

[16] R. Burgos, A. Uan-Zo-li, F. Lacaux, A. Roshan, F. Wang, and D. Boroyevich, "New step-up and step-down 18-pulse direct asymmetric autotransformer rectifier units," in *Proc. IEEE 36th Conf. Power Electron. Spec.*, Nov. 2015, pp. 1–6.

[17] J. Chen, C. Gong, and J. Chen, "Application of multi-pulse rectification technology in wind power generation," *Trans. China Electrotech. Soc.*, vol. 27, no. 4, pp. 131–137, Aug. 2012.

XIAOQIANG CHEN received the Ph.D. degree from the School of Electrical Engineering and Automation, Lanzhou Jiaotong University, Lanzhou, in 2010. He is currently a Professor with the School of Electrical Engineering and Automation, Lanzhou Jiaotong University. His research interests include high-power special type power supply and its application, energy storage systems.

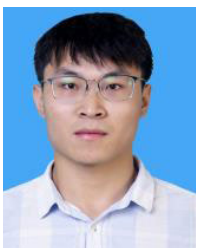

TAO CHEN received the B.S. degree in electrical engineering and its automation from Dalian Jiaotong University, Liaoning, China, in 2019. He is currently pursuing the M.S. degree in electrical engineering with Lanzhou Jiaotong University, Lanzhou, China. His research interests include power quality transformation and control, and multi-pulse rectification and its harmonic suppression.

YING WANG received the B.S. degree from the School of Electrical Engineering and Automation, Chongqing University, Chongqing, China, and the Ph.D. degree from the School of Electrical Engineering, Southwest Jiaotong University, Chengdu, China. His main research interests include high power converters and harmonics compensation.